Water Research 186 (2020) 116346

Contents lists available at ScienceDirect

Water Research

journal homepage: www.elsevier.com/locate/watres

Haloacetonitriles and haloacetamides precursors in filter backwash and sedimentation sludge water during drinking water treatment

Yunkun Qian[a], Yue Hu[a], Yanan Chen[a], Dong An[a,e,*], Paul Westerhoff[b], David Hanigan[c], Wenhai Chu[d,e]

[a] Department of Environmental Science & Engineering, Fudan University, Shanghai 200238, China
[b] School of Sustainable Engineering and the Built Environment, Ira A. Fulton Schools of Engineering, Arizona State University, Tempe, AZ 85287-3005, United States
[c] Department of Civil and Environmental Engineering, University of Nevada, Reno, NV 89557-0258, United States
[d] State Key Laboratory of Pollution Control and Resources Reuse, National Centre for International Research of Sustainable Urban Water System, College of Environmental Science and Engineering, Tongji University, Shanghai, 200092, China
[e] Shanghai Institute of Pollution Control and Ecological Security, Shanghai 200092, China

ARTICLE INFO

Article history:
Received 20 May 2020
Revised 27 July 2020
Accepted 23 August 2020
Available online 23 August 2020

Keywords:
Filter backwash water
Sedimentation sludge water
Haloacetonitriles
Haloacetamides, disinfection byproducts

ABSTRACT

Haloacetonitriles (HANs) and haloacetamides (HAMs) are nitrogenous disinfection byproducts that are present in filter backwash water (FBW) and sedimentation sludge water (SSW). In many cases FBW and SSW are recycled to the head of drinking water treatment plants. HAN and HAM concentrations in FBW and SSW, without additional oxidants, ranged from 6.8 to 11.6 nM and 2.9 to 3.6 nM of three HANs and four HAMs, respectively. Upon oxidant addition to FBW and SSW under formation potential conditions, concentrations for six HANs and six HAMs ranged from 92.2 to 190.4 nM and 42.2 to 95.5 nM, respectively. Therefore, at common FBW and SSW recycle rates (2 to 10% of treated water flows), the precursor levels in these recycle waters should not be ignored because they are comparable to levels present in finished water. Brominated HAN and chlorinated HAM were the dominant species in FBW and SSW, respectively. The lowest molecular weight ultrafiltration fraction (< 3 kDa) contributed the most to HAN and HAM formations. The hydrophilic (HPI) organic fraction contributed the greatest to HAN precursors in sand-FBW and SSW and were the most reactive HAM precursors in both sand- or carbon-FBWs. Fluorescence revealed that aromatic protein-like compounds were dominant HAN and HAM precursors. Therefore, strategies that remove low molecular weight hydrophilic organic matter and aromatic protein-like compounds will minimize HAN and HAM formations in recycled FBW and SSW.

1. Introduction

Coagulation, sedimentation, and filtration are the primary unit operations to remove dissolved organic matter in drinking water treatment plants (DWTPs). Large volumes of filter backwash water (FBW) and sedimentation sludge water (SSW) are produced during water treatment, accounting for approximately 2–10% of total water flow in DWTPs (Shafiquzzaman et al., 2018; Walsh et al., 2008). Suspended solids, natural organic matter (NOM), disinfection byproduct (DBP) precursors, bacteria, and inorganic metals (e.g., Fe, Mn, and Al) are present in abundance in FBW and SSW (Chen et al., 2015; Mccormick et al., 2010). Recycling of partially-treated FBW or supernatant from SSW treatment is common at DWTPs to maximize efficiency. In China, FBW and SSW are usually treated only via thickener-induced precipitation prior to discharging the supernatant to surface waters, impacting receiving ecosystems. In response to economic development concerns stemming from adverse impacts of surface water discharges, new standards for FBW and SSW discharge were recently issued in China. Therefore, FBW and SSW recycling has attracted considerable interest not only to reduce receiving-water pollution but also to improve net water production rates within DWTPs (Bourgeois et al., 2004). In the USA, FBW and SSW are typically pumped to intermittent storage tanks, where much of the solids precipitate, before being recycled and blended with incoming raw water at the head of the DWTPs (Tobiason et al., 2003). Recent work showed that recycling sludge supernatant containing polymer residuals and preformed DBPs contributes to one specific DBP class (nitrosamines) that eventually impacts DBPs in treated drinking water (Westerhoff et al., 2019). While characteristics of natural organic

* Corresponding author.
E-mail address: andong@fudan.edu.cn (D. An).

https://doi.org/10.1016/j.watres.2020.116346
0043-1354/

matter (NOM) that serve as precursors for unregulated DBPs have been well studied in source water (Ersan et al., 2019; Krasner et al., 2013), little is known about the nature of organic material (unregulated DBPs or DBP precursors) in FBW or SSW that are recycled to the head of DWTPs (Mccormick et al., 2010; Tan et al., 2017).

All disinfectants react with NOM in water to form DBPs, some of which are potential or known human carcinogens (Ackerson et al., 2018; An et al., 2019; Plewa et al., 2002, 2009). More than 600 DBPs have been identified in water, including trihalomethanes (THMs), haloacetic acids (HAAs), haloacetonitriles (HANs), and haloacetamides (HAMs) (Chen et al., 2010; Plewa et al., 2008a; Richardson et al., 2007, 2011; Vu et al., 2018). HANs and HAMs are nitrogenous DBPs with substantially greater cytotoxicity and genotoxicity than THMs and HAAs (Karanfil et al., 2008; Muellner et al., 2007; Plewa et al., 2008b). HANs and HAMs are typically present at lower concentrations than THMs and HAAs, but they still contribute, in many cases, the greatest to overall toxicity of a treated water sample (Y.H. Chuang et al., 2019; Dad et al., 2018; Komaki et al., 2014; Plewa et al., 2010; Wagner et al., 2017). HANs and other emerging DBPs are predicted to exert the majority of the DBP-related toxicity risk in drinking water (Cuthbertson et al., 2019; Kimura et al., 2019; Krasner et al., 2016). HANs and HAMs (primarily dichloroacetonitrile (DCAN) and 2,2-dichloroacetamide (DCAM)) have been frequently detected in raw, drinking, and reuse water sources (Liew et al., 2012; Krasner et al., 2006). For instance, six HAM species were detected in drinking water in Japan (Kosaka et al., 2016), three HAM species were detected in drinking water in England (Bond et al., 2015), four HAN and HAM species were detected in reuse water in the U.S. (Zeng et al., 2016), and four HAN and HAM species were detected in drinking water in China (Huang et al., 2017). Because of their high toxicity and occurrence, strategies to control HAN and HAM formations relative to other DBPs are emerging as an important research area (Krasner et al., 2006; McKenna et al., 2020).

Removing HAN and HAM precursors before disinfection is more practical than removing the associated DBPs after formation because they are nonvolatile, rendering practical methods such as air stripping ineffective (Hanigan et al., 2012; Jiang et al., 2017). NOM is composed of a complex mixture of heterogenous organic compounds, which act as DBP precursors (Krasner et al., 2018; Yang et al., 2012). The organic composition and the chemical structure of NOM in-plant recycled water are more complex and at higher concentration than in raw and treated drinking water (Krasner et al., 2009). Studies have shown that recycled FBW and SSW water increases formation of selected DBPs, although the number of studies is few, and there are even fewer studies of the recycled precursors (Hou et al., 2016; Tan et al., 2017). Therefore, to control DBP formation during in-plant recycling in DWTPs, it is necessary to better understand the physicochemical properties of NOM in reuse water.

Molecular weight (MW) distribution and hydrophilicity of NOM are common tools used to characterize DBP precursors (Finkbeiner et al., 2020; Wang et al., 2013; Xu et al., 2007). Low MW compounds (<3 kDa) often disproportionately contribute to DBP formation (An et al., 2017, 2019; Hua et al., 2007). Synthetic resins (e.g., XAD®−4 and XAD®−8) are used to fractionate NOM into hydrophilic (HPI), transphilic (TPI), and hydrophobic (HPO) fractions (Fabris et al., 2008; Golea et al., 2017; Hanigan et al., 2013). In the USA, Australian, Norwegian, UK, and Japan, HPO fraction was the most dominant part of NOM in the source water (Fabris et al., 2008; Finkbeiner et al., 2020; Golea et al., 2017; Hanigan et al., 2013; Hua et al., 2007; Phetrak et al., 2016). In China, Canada, and Turkey, HPI fraction was the dominant NOM in source water (Chu et al., 2010; Hu et al., 2016; Karapinar et al., 2014; Lamsal et al., 2012; Xu et al., 2007; Wang et al., 2013). The characteristics of DOM fractions may be due to industrial contaminants, DOM origins, catchment geochemistry, rainfall and other factors. Croué et al. (2000) showed that the HPO fraction provided the most reactive THM and HAA precursors at least for the studied water source. Chu et al. (2010) found that HPI organic material had the highest DCAM reactivity in a major DWTP source water of China. These results indicate that different water sources and different NOM fractions contain varying DBP precursors.

The goal of this research was to characterize and quantify HAN and HAM precursors in FBW and SSW recycled water from two DWTPs. HAN and HAM precursors were characterized using MW and hydrophilicity fractionation plus fluorescence spectral analysis to relate DBP formation to NOM reactivity. Potential treatment methods are also discussed to lessen the DBP impact from FBW and SSW recycling.

2. Materials and methods

2.1. Water sample collection

Water samples were collected from two DWTPs (i.e., DWTP-A and DWTP-B) in Shanghai, China. Water samples were collected in pre-cleaned 5 L glass bottles, and residual chlorine was quenched by immediately adding sodium thiosulfate. All samples were stored at 4 °C in ice boxes after being filtered by a 0.45 μm glass fiber filter. Additional details on water sources and sampling are provided in Supplemental Information.

2.2. Chemical reagents

Pure DBP standards in solvents included HANs (chloroacetonitrile (CAN), bromoacetonitrile (BAN), dichloroacetonitrile (DCAN), bromochloroacetonitrile (BCAN), trichloroacetonitrile (TCAN), dibromoacetonitrile (DBAN), and iodoacetonitrile (IAN)) and HAMs (2-chloroacetamide (CAM), 2-bromoacetamide (BAM), dichloroacetamide (DCAM), bromochloroacetamide (BCAM), trichloroacetamide (TCAM) and dibromoacetamide (DBAM)), which were purchased from Dr. Ehrenstorfer (Augsburg, Germany). High performance liquid chromatography (HPLC) grade methyl *tert*–butyl ether (MTBE) and anhydrous sodium sulfate (Na_2SO_4, analytical research grade, 99%) were supplied by Sigma Aldrich (St. Louis, MO, USA). Ultrapure water was prepared using a Gradient A10 ultrapure water system (Milli-Q®, Millipore Corporation, Bedford, MA, USA). Other reagents (analytical grade) were purchased from Sigma Aldrich.

2.3. Chlorination of water samples

HAN and HAM formation potential (FP) tests were performed according to the methods detailed in Krasner et al. (2006). Briefly, water samples were chlorinated at 25 °C for 72 h in the dark at pH 7 (20 mM phosphate buffer solution). Chlorine dose for the DBP FP tests was calculated by Eq. (1). Residual chlorine was quenched using excess sodium thiosulfate. Samples were then analyzed for HANs and HAMs. HAN and HAM FPs in different water samples were calculated according to Eqs. (2) and (3).

$$Cl_2\,dose(mg/L) = 3 \times DOC(mg\,C/L) + 7.6 \times NH_3(mg\,N/L) + 10 \quad (1)$$

$$C_{(HAN\ FP)} = C_{(HAN)}(after\ chlorination) - C_{(HAN)}(before\ chlorination) \quad (2)$$

$$C_{(HAM\ FP)} = C_{(HAM)}(after\ chlorination) - C_{(HAM)}(before\ chlorination) \quad (3)$$

2.4. Fractionation and characterization of HAN and HAM precursors

2.4.1. MW fractionation

Water samples were fractionated into nominal MW fractions of < 3, < 10, and < 100 kDa fractions by a MinimateTM II tangential flow filtration (TFF) system (Pall Corporation, USA) using Ultracel®-PL ultrafiltration (UF) membranes (Millipore Sigma, USA). Measurements were performed on both fractionated and raw water samples to conduct mass balances (additional information provided in Supplemental Information). DOC concentrations in fractionated water samples and different MW fractions are shown in Table S1 and S2. The concentrations in MW fractions were obtained either directly (e.g., < 3 kDa) or by subtraction (e.g., concentration in 3 to 10 kDa fraction equal to that measured in the < 10 kDa filtrate minus the concentration in the < 3 kDa filtrate).

2.4.2. Hydrophilicity fractionation

XAD®−4 and XAD®−8 nonionic resins (AmberLiteTM, DuPont, Inc., USA) were used to fractionate water samples into XAD®−4 and XAD®−8 components. The concentrations of the HPI, TPI, and HPO fractions were obtained by subtraction from the non-fractionated samples (additional information provided in Supplemental Information).

2.4.3. EEM spectral analysis

Fluorescence excitation-emission matrix (EEM) spectra were measured using a fluorescence spectrophotometer (Cary Eclipse, Agilent Technologies, USA). The excitation wavelength (λ_{Ex}) was varied from 200 to 500 nm, and emission (λ_{Em}) was varied from 250 to 600 nm, each in 10 nm increments. Slit widths of the excitation and emission monochromators were set at 5 nm, and scan speed was set to 1200 nm/min.

Using a analytical approach termed fluorescence regional integration (FRI), the EEM spectra were divided into five regions representing specific organic matter components Chen et al., 2003): region I (representing aromatic protein-like compounds such as tyrosine, λ_{Ex} < 250 nm, λ_{Em} < 330 nm); region II (representing aromatic protein-like compounds such as tryptophan, λ_{Ex} < 250 nm, λ_{Em} < 380 nm); region III (representing fulvic acid-like compounds, λ_{Ex} <250 nm, λ_{Em} > 380 nm); region IV (representing soluble microbial products including tryptophan-like and biologically-related tyrosine-like compounds, λ_{Ex} > 250 nm, λ_{Em} < 380 nm); and region V (representing humic acid-like compounds, λ_{Ex} > 250 nm, λ_{Em} > 380 nm). The integral volume (Φ_i) of a specific fluorescent region was calculated and normalized to the volume of the full EEM, resulting in an integrated standard volume ($\Phi_{i,n}$) of the specific fluorescent region. Relevant calculations are given by Eqs. (4)-((7).

$$\Phi_i = \int_{exem}\int \mathrm{I}(\lambda_{ex}\lambda_{em})\mathrm{d}\lambda_{ex}\mathrm{d}\lambda_{em}, \quad (4)$$

$$\Phi_{i,n} = \mathrm{MF}_i\Phi_i, \quad (5)$$

$$\Phi_{\mathrm{T,n}} = \sum \Phi_{i,n}, \quad (6)$$

$$P_{i,n} = \Phi_{i,n}/\Phi_{\mathrm{T,n}} \times 100\%, \quad (7)$$

Where $\mathrm{I}(\lambda_{ex}\lambda_{em})$ is fluorescence intensity (au) at each excitation-emission wavelength pair, $\Phi_{\mathrm{T,n}}$ is total fluorescence area integrated to produce a volume (au·nm^2), MF_i is a multiplication factor equal to the ratio of total integrated area to the i^{th} integrated fluorescence area, and $P_{i,n}$ is proportion of the i^{th} integrated volume to the total integrated standard volume of the fluorescence area (%).

2.5. Analytical methods

Seven HANs and six HAMs were analyzed by liquid-liquid extraction (LLE) and gas chromatography (GC, 7890B, Agilent Technologies, USA) equipped with a 30 m × 0.25 mm × 0.25 μm DB-1701 column (J&W Scientific, USA) and an electron capture detector (ECD, Agilent Technologies, USA). HAN and HAM quantification methods are described in Supplemental Information.

Dissolved organic carbon (DOC) and dissolved nitrogen (DN) of filtered solutions were measured by a total organic carbon (TOC) analyzer (Multi N/C 2100, Analytik Jena AG, Germany). Dissolved organic nitrogen (DON) was calculated by subtracting nitrate, nitrite, and ammonia concentrations from the DN concentration (APHA, 2005). Free and total chlorine concentrations were measured by the *N,N*–diethyl–*p*-phenylenediamine (DPD) powder pillow photometric method (APHA, 2005). Bromide incorporation factors (BIFs, the fractional extent of bromination of the methyl group) for HAN and HAM were calculated as shown in Supplemental Information. The experimental process for MW and hydrophilicity fractionations and analyses were conducted in triplicate.

3. Results and discussion

3.1. Water quality

Table 1 shows the water quality characteristics for FBW and SSW from the two DWTPs. Both plants use sand filters and generate sand-filter backwash water (sand-FBW). Additionally, DWTP-B also has a granular activated carbon filter that generates carbon-filter backwash water (carbon-FBW). SSW contained 2.7–5.8 mg-DOC/L and 0.28–0.46 mgDON/L. These concentrations were higher than the DOC and DON in FBW (Table 1). Aromaticity, as measured by SUVA, was greater in the FBW than the SSW. Bromide was up to 4x higher in the SSW than the FBW. Collectively, the higher organic matter and bromide in SSW samples suggests they have greater potential to form DBPs compared with FBW samples.

3.2. HAN, HAM, and precursor concentrations

3.2.1. HANs and HAMs

Fig. 1 shows preformed HAN and HAM in FBW and SSW. Total HANs were greater in FBW (6.8–11.6 nM) than SSW (2.9–3.6 nM). Among the seven HANs, BCAN was the most prevalent, at 3.6–4.1 nM and 2.9–3.6 nM in FBW and SSW, respectively.

Finished water containing free chlorine is used to backwash the sand and carbon filters. Therefore, HANs in the FBW form in the finished water before backwashing and also react with organic matter in filters (Fig. S3a). HAN concentrations and speciation in sand- and carbon-FBWs were different than the finished water, indicating that HANs were primarily generated by reactions between the residual disinfectant with organic matter in the filter, while a small fraction (15%–18%) was from the finished water (Fig. S3c).

Total HAMs were 5.3–10.5 nM and 2.3–9.9 nM in FBW and SSW, respectively. Among the six HAMs, DCAM was present at the highest concentration across all samples and both treatment plants, which is consistent with another study of HAMs in recycled water from 12 DWTPs in Japan (Kosaka et al., 2016). Other HAM species (i.e., CAM, BAM, and BCAM) were present only at very low concentrations. HAM concentrations in sand- and carbon-FBWs were higher than in SSW, which were similar to concentrations in raw water (Fig. S3 (b)). Notably, the concentrations of the few DBPs present in the raw water were somewhat greater than the finished waters (Fig. S3), suggesting that the source waters are polluted at low levels with chlorinated and brominated organic matter, and that the treatment plants removed at least some of these compounds.

Table 1
Water quality characteristics. Error represents the standard deviation of triplicates.

Parameters	DWTP-A		DWTP-B		
	Sand-FBW	SSW	Sand-FBW	SSW	Carbon-FBW
Ph	7.7 ± 0.0	7.8 ± 0.0	7.6 ± 0.0	7.8 ± 0.0	7.6 ± 0.1
Turbidity (NTU)	6.9 ± 0.2	17.7 ± 0.3	6.0 ± 0.2	23.2 ± 1.7	8.1 ± 0.4
DOC (mgC/L)	1.7 ± 0.2	2.7 ± 0.2	2.3 ± 0.0	5.8 ± 0.0	2.7 ± 0.1
UV_{254} (cm^{-1})	0.04±0.00	0.05±0.00	0.04±0.00	0.06±0.00	0.06±0.00
SUVA (L/mg·m)	2.1 ± 0.5	2.0 ± 0.1	1.6 ± 0.1	1.1 ± 0.1	2.1 ± 0.2
DON (mgN/L)	0.20±0.01	0.28±0.01	0.22±0.02	0.46±0.03	0.21±0.02
Br^- (μg/L)	214±2	885±6	114±4	160±2	105±4

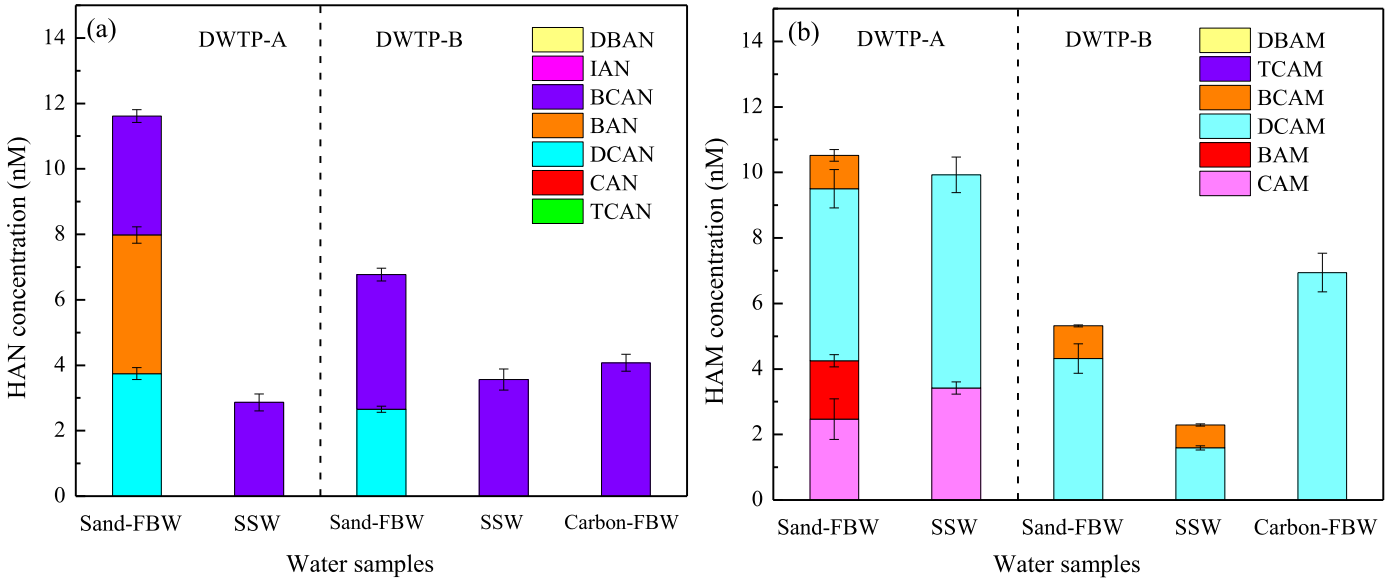

Fig. 1. (a) HAN and (b) HAM concentrations in FBW and SSW. Error bars represent one standard deviation (n = 3).

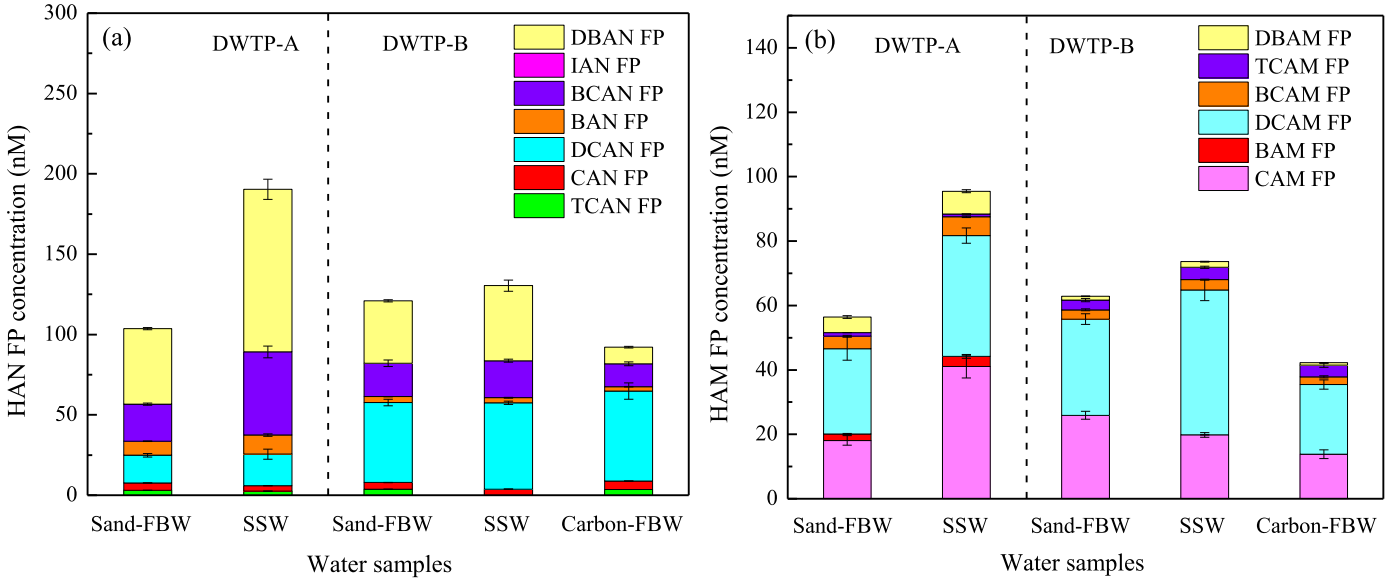

Fig. 2. Precursors of (a) HANs and (b) HAMs in FBW and SSW. Error bars represent one standard deviation (n = 3).

3.2.2. HAN and HAM precursors

Fig. 2a and 2b show HAN and HAM formation potentials in FBW and SSW, which are higher in SSW than sand- or carbon-FBWs. This is likely due to more DOM being present in SSW than in FBW, and there was a linear correlation between HAN FP and DON (R^2 = 0.92, $p < 0.05$, DWTP-A; R^2 = 0.99, $p < 0.05$, DWTP-B) when data were aggregated from raw water, SSW and FBW (Fig. 3a and 3b). This indicates that NOM, particularly DON, were the major sources of HAN and HAM precursors. Fig. 3c shows that HAN FP strongly correlated with HAM FP (R^2 = 0.94, $p < 0.05$), suggesting that both of these N-DBPs may originate from a common precursor pool. Another reason may have been the hydrolysis

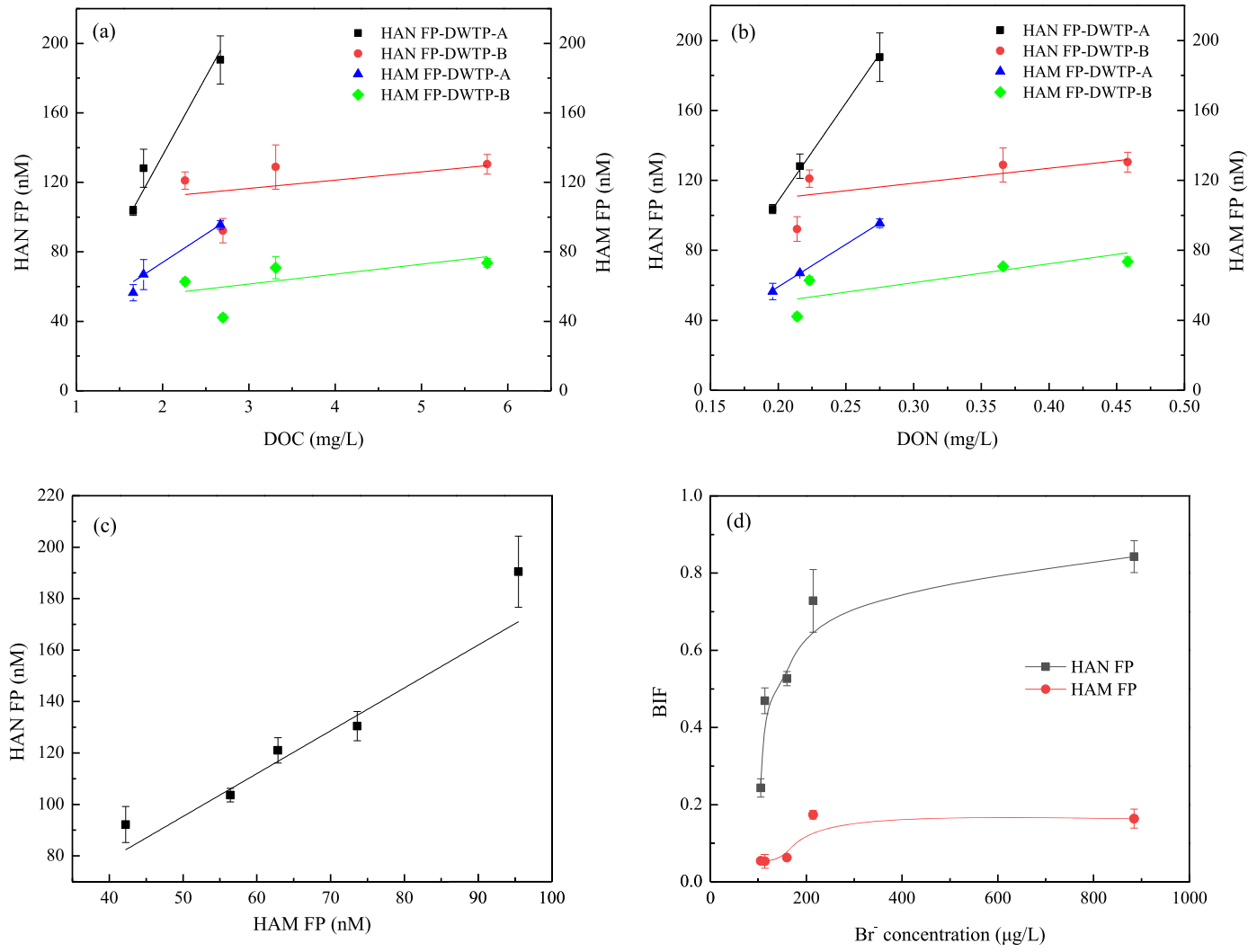

Fig. 3. Relationships between (a) HAN and HAM FPs and DOC, (b) HAN and HAM FPs and DON, (c) HAN and HAM FPs, and (d) BIF and bromide. Error bars represent one standard deviation ($n = 3$).

of HANs to HAMs (Huang et al., 2012). Among the seven HANs, only iodoacetonitrile (IAN) was not detected after chlorination, and DBAN formed to the greatest extent in all samples except for carbon-FBW. HAN formation can be influenced by bromide concentration because hypobromous acid (HOBr) preferentially substitutes the halogen atom more than HOCl (Allard et al., 2015; Westerhoff et al., 2004). DBAN is one of the most cyto- and genotoxic HANs for which data are available (Wagner et al., 2017) and DBAN (38.9–101.2 nM) was formed during FP tests, but not formed at detectable levels in the treatment plant from reactions with residual disinfectant. This may be attributable to the much lower concentrations formed in the plant, where DBAN may have formed, but at levels that were below the detection limit. As expected, bromide incorporation factors (BIFs) of HANs and HAMs increased with increasing bromide concentrations, although a similar trend was not observed for HANs (Fig. 3d). SSW formed more HANs than FBW, which could be associated with the bromo–haloacetonitriles (Br-HANs) production. In SSW, Br-HANs were 73–147 nM, which was higher than FBW (27–79 nM).

Total HAM FP ranged from 56.4 to 62.9 nM and 73.6 to 95.5 nM in FBW and SSW, respectively (Fig. 2b). Cl-HAM FPs were higher than Br-HAM FPs in FBW and SSW, despite a strong relationship between Br^- and HAM FP. This is similar to the findings reported by Chu et al. (2013) in Lake Tai water (China), where the Cl-HAM was the main HAM during chlorination.

3.3. Fractionation and characterization of HAN and HAM precursors

3.3.1. MW distribution

Low MW (< 3 kDa) organic material was the primary DOM in nearly all samples, regardless of treatment plant or unit process. The DOC in this fraction accounted for > 40% of the total DOC (Fig. 4a and b). In SSW collected from DWTP-B, the > 100 kDa fraction also contributed 42% of the total DOC.

Fig. 4 also shows HAN and HAM FPs from the fractionated DOM. The fraction with MW < 3 kDa contributed the greatest amount of HAN and HAM precursors in all samples, accounting for 47–75% and 58–78% of the nonfractionated FPs, which indicates that low MW organic matter was the primary HAN and HAM precursor. This finding agrees with previous results by Huang et al. (2016), who found the low MW compounds had the greatest DCAM yields, accounting for more than 54% of the FP. The low MW fraction (< 3 kDa) also had the greatest Br-HAN and Br-HAM FPs in all samples, accounting for 61–79% and 66–87% of total Br-HAN and Br-HAM formation, respectively. Because the MW fractionation had little impact on the bromide concentration (Table S3), the < 3 kDa

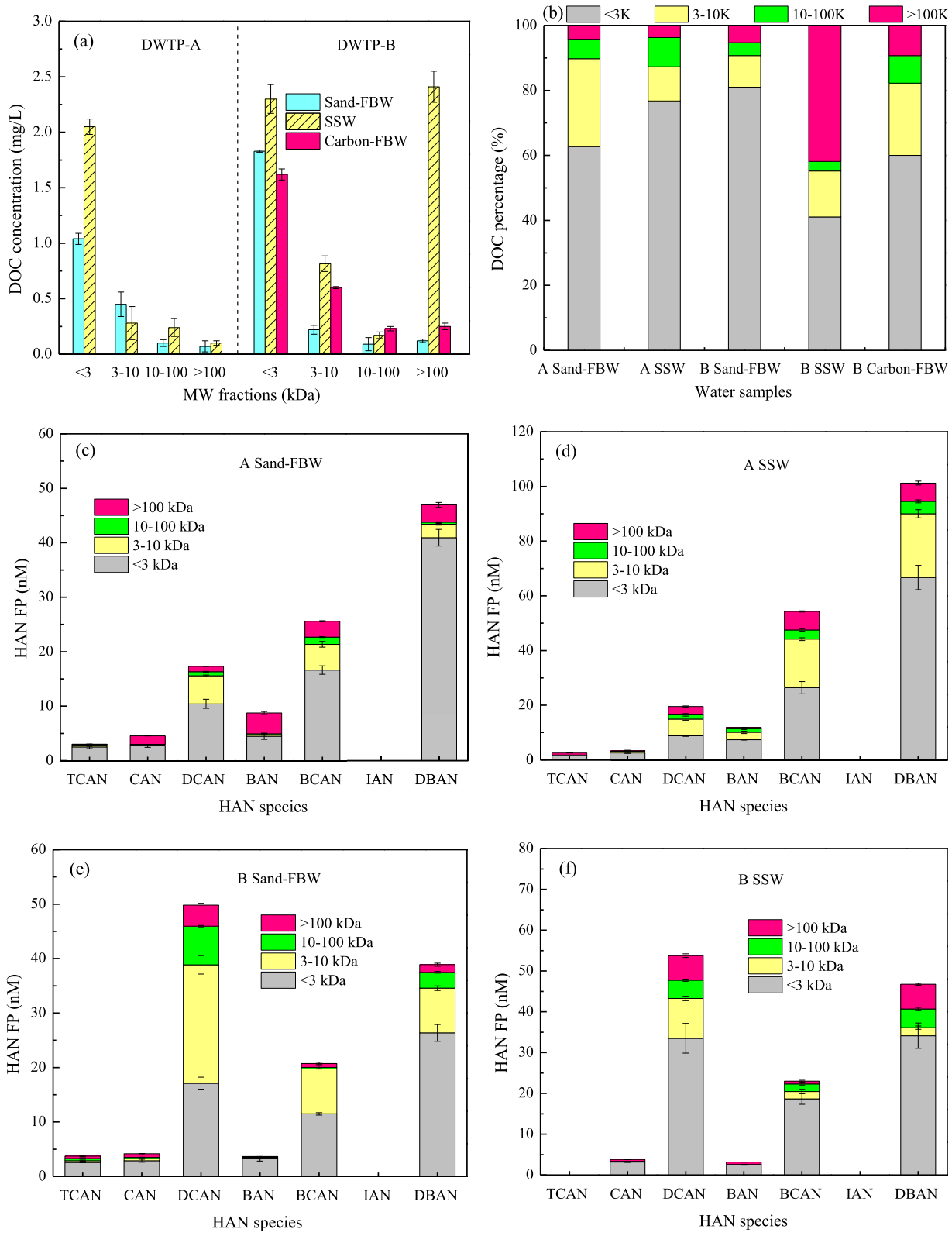

Fig. 4. DOC (a) concentrations and (b) percentages and (c-g) HAN and (h-l) HAM FPs in different MW fractions. Error bars represent one standard deviation (n = 3).

fraction had a greater bromide to DOC ratio, which likely influenced formation of Br-DBPs.

3.3.2. Hydrophobic and hydrophilic distributions

Figs. 5a and 5b show that the HPI fraction accounted for more than 54% of total DOM in all samples except carbon-FBW. Carbon-FBW contained more HPO components (52%), potentially due to the enriched microorganisms in carbon filter that produced HPO soluble microbial products (Zheng et al., 2018), which were subsequently washed into the FBW.

The highest HAN concentrations formed from the HPI fraction in sand-FBW and SSW. More than 57% of total HAN formation

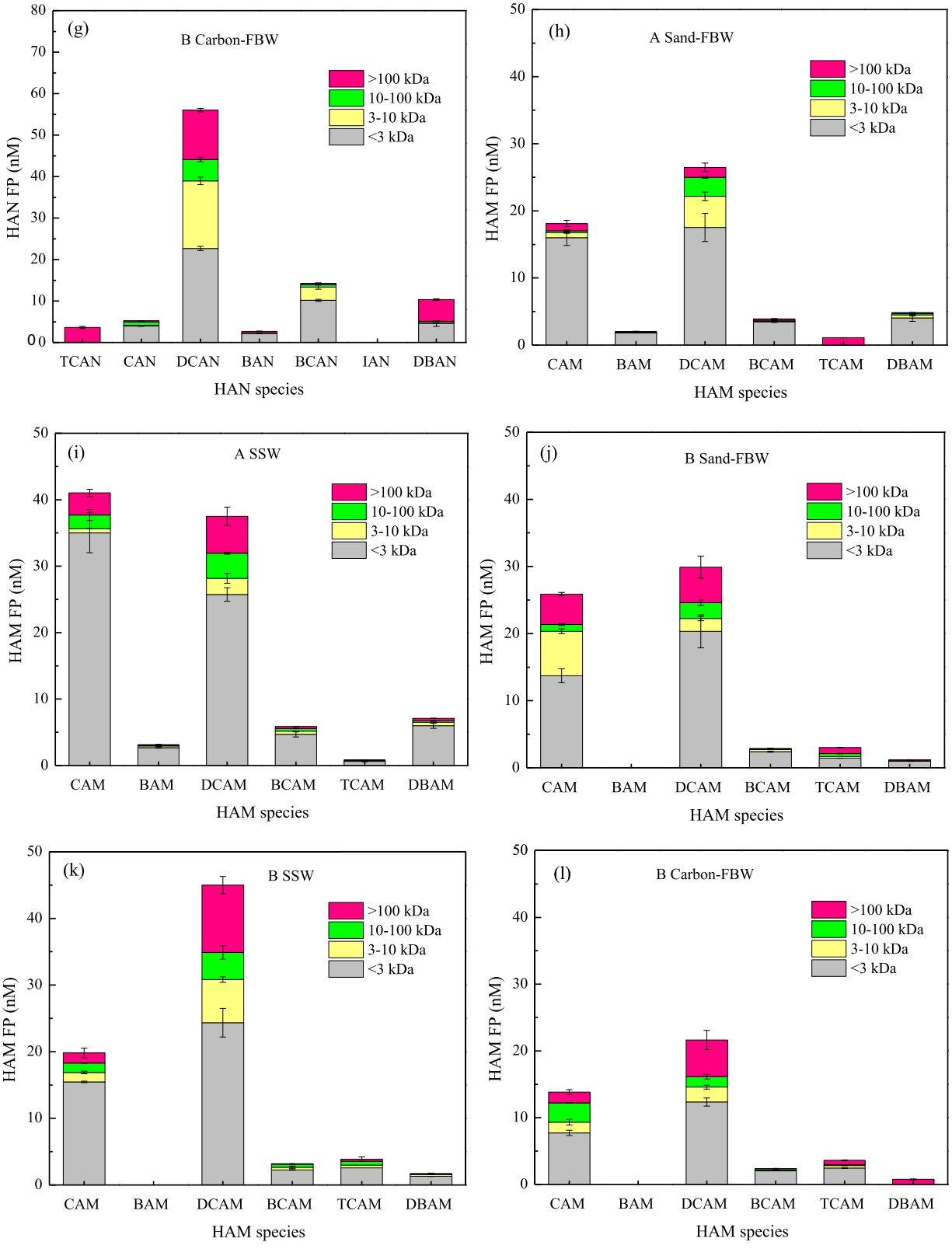

Fig. 4. Continued

was attributable to the HPI fraction, indicating that HPI organics were the primary HAN precursors in sand-FBW and SSW. On a DOM-normalized basis, HPI organic matter from the sand-FBW and SSW in DWTP-A formed 53.8 and 58.1 nmolHAN/mgC, respectively, compared with 338 and 108 nmolHAN/mgC formed from the respective HPO fractions (Fig. S4a). This suggests that the HPO fraction is more reactive in forming HANs. The opposite result was found in DWTP-B (i.e., the HPI fraction was more reactive). In the carbon-FBW, HPI and HPO fractions formed almost the same HAN after chlorination, which was opposite to the observed trend for

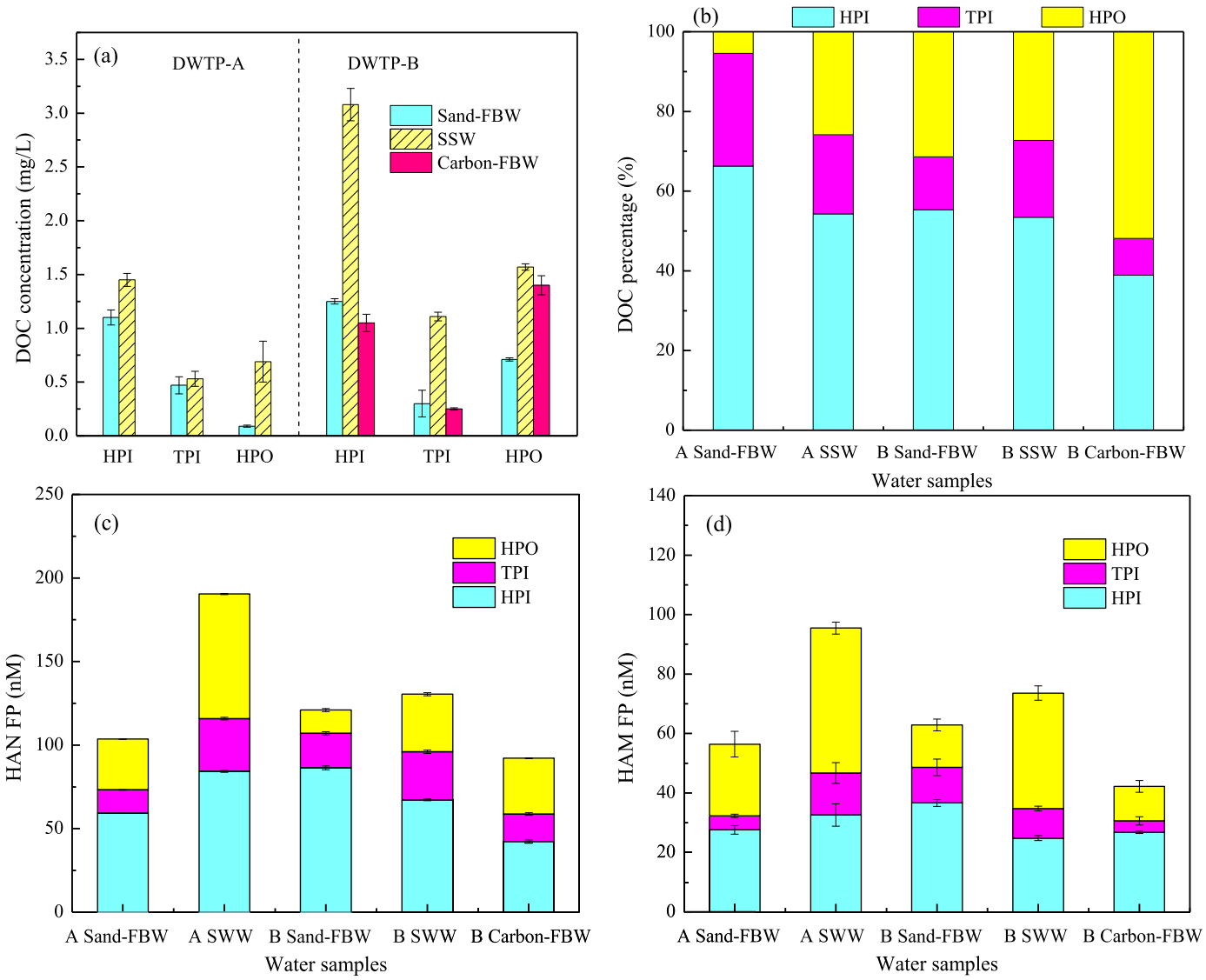

Fig. 5. DOC (a) concentration, (b) percentage, (c) HAN and (d) HAM FPs in different hydrophilicity fractions. Error bars represent one standard deviation ($n = 3$).

DOC. Br-HANs were primarily produced by HPI organic matter, suggesting that HPI organic matter contained more aliphatic organic matter and was more reactive with HOBr than HOCl in forming Br-HANs (Hua et al., 2007). Alternatively, the greater reactivity of the HPI fraction in forming Br-DBPs may be at least partially attributable to the fractionation technique, where Br^- is not present in the HPO fraction.

For HAM FPs, the HPI fraction had the most HAM precursors, more than 49% for the sand- and carbon-FBWs. The HPO fraction in SSW contained 51% of the HAM precursors. Other fractions represented < 49%. These two opposing results indicate that HPI organic matter was the primary source of HAM precursor in sand- and carbon-FBWs and, conversely, that HPO organic matter dominated the HAM precursor pool in SSW. The results of DOM normalization showed that the HPO fraction was more reactive in forming HAMs in DWTP-A (Fig. S4b). Higher Br-HAM FPs in the HPO fraction indicated that some HPO organic matter was more easily oxidized to HAMs than HANs by HOBr.

3.3.3. EEM spectra

Area volumes ($\Phi_{i,n}$) from the EEM spectra are shown in Fig. 6. The corresponding EEM fluorescence spectra is provided in Fig. S5. Sand-FBW and SSW EEM spectra exhibited high intensities in region II, with corresponding area volumes for 35–38% and 32–42%, respectively, of all the sum of all the regional volumes. Region II contributed an even greater proportion of the EEM volume for the carbon-FBW sample, up to 48%. This region is typically associated with aromatic protein-like compounds and indicates that they were a large component of DOM in FBWs and SSWs.

Figs. 6c and 6d show that the MW < 3 kDa fraction had the greatest intensity volume, more than 64% of the total volume, which is similar to the proportion of DOC, HAN, and HAM FPs in this fraction (41–81% of DOC, 48–80% of HAN, and 59–75% of HAM). HPI and HPO fractions contributed the greatest amount to region II intensity volumes.

There was not a strong linear correlation between regional area volumes and HAN FP and HAM FP, likely because the HAN and HAM formations were impacted more strongly by bromide (Fig. 3c). The correlations between region II area volumes and HAN FP ($R^2 = 0.32$, $p < 0.05$) and between region I area volumes and HAM FP ($R^2 = 0.63$, $p < 0.05$) were better than other regions ($R^2 < 0.3$, $p < 0.05$) (Fig. S7), indicating that aromatic protein-like compounds may play a greater role as HAN and HAM precursors than other regions and associated functional groups. The close

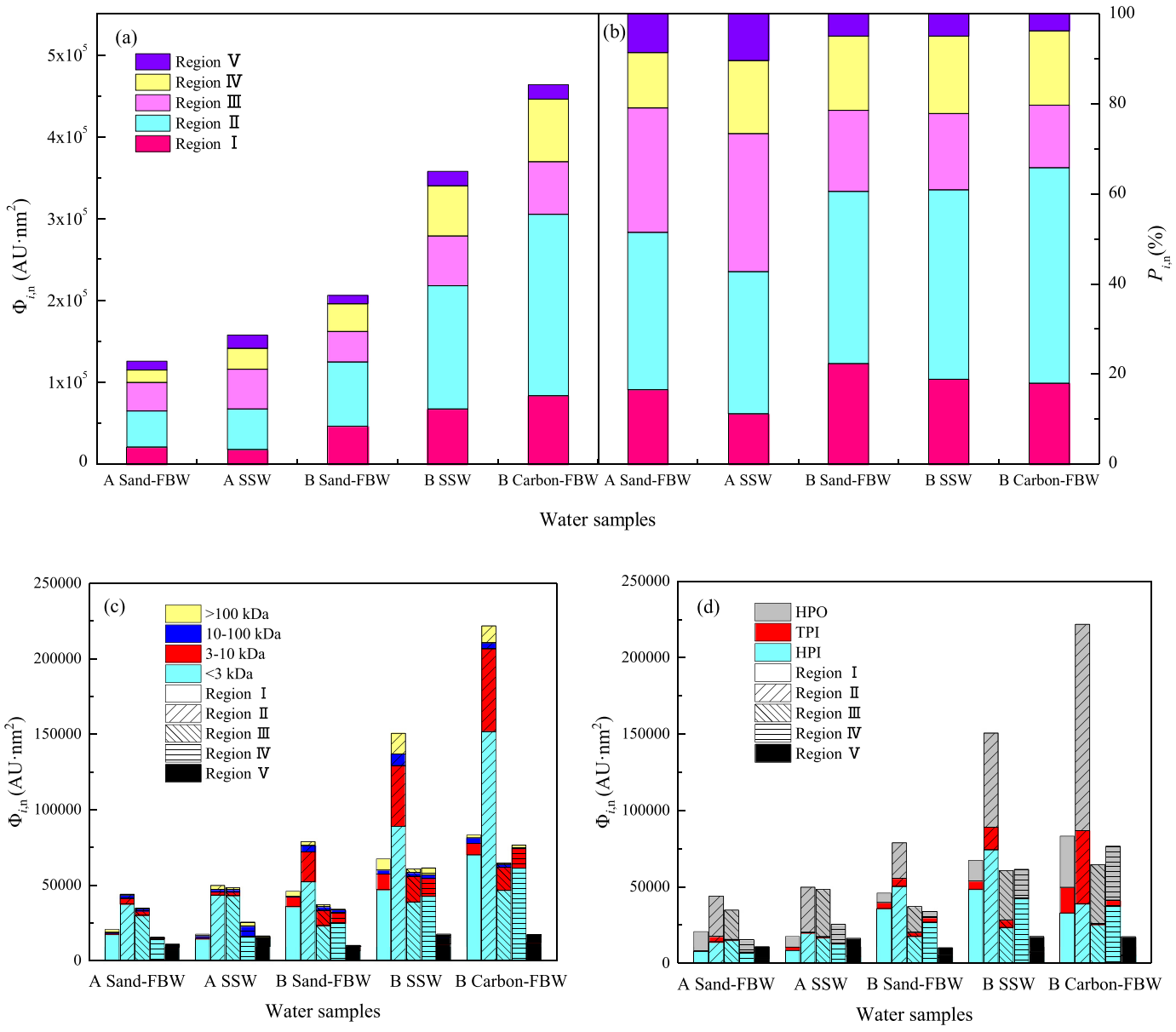

Fig. 6. FRI EEM spectra generated for SSW and FBW samples [(a) and (b)] and different MW and hydrophilicity fractions [(c) and (d)].

association between the findings for region I and II, MW fractionation, and hydrophobicity fractionation (Fig. S7), combined with FP results suggests that low MW, HPO/HPI aromatic protein-like compounds are likely to be the largest source of HAN and HAM precursors in FBWs and SSWs.

3.4. Backwash treatment options

Due to the variable water quality across treatment plants, there is no single water treatment method suitable for the reuse of all FBW and SSW. Low MW and HPI organics have been shown to be the primary HAN and HAM precursors in FBW and SSW but both conventional water treatment processes and advanced treatment process es are more effective at removing the high MW and HPO organic matter (Chiu et al., 2012; Hanigan et al., 2015; Wang et al., 2017). Therefore, attention should be focused on permanent removal of low MW, HPI organic matter because of its contribution to HAM and HAN formation and because it is not well removed by current water treatment techniques. Activated carbon removes HPO matter well and removes some HPI matter, and would likely result in reduced HAM and HAN formation from the SSW and FBWs. But there is conflicting evidence as to whether activated carbon produces water that has an overall toxicity that is less than the untreated samples, particularly for samples with high bromide, due to greater rejection of DOC than of bromide (Ates et al., 2009; Cuthbertson et al., 2019, 2020; McKenna et al., 2020; Krasner et al., 2016). Other alternatives are likely to be more energy and cost intensive. For example, coagulation combined with UF removes DOM from water well but is energy intensive well but is energy intensive (Qian et al., 2011). Advanced oxidation processes (AOPs), especially UV/H_2O_2 and UV/Cl_2, have been proven effective for degrading NOM, especially low MW and HPI organics, through formation of highly reactive radicals (Y.H. Chuang et al., 2019; Zhang et al., 2019). It has also been shown that cytotoxicity and genotoxicity were reduced by combined UV plus chlorine (Plewa et al., 2012), but again, these methods are energy intensive. Thus, it may be the most cost effective to consider strategies to either sequester bromide from FBW and SSW, or to optimize coagulation

strategies which result in limited bromide accumulation in the FBW and SSW.

4. Conclusion

This research provides information and analyses on the HAN and HAM concentrations and precursors in FBW and SSW in DWTPs. Total HAN precursor loading in FBW and SSW resulted in 92.2–190.4 nM, meanwhile, total HAM precursor loading in FBW and SSW resulted in 42.2–95.5 nM. DBAN precursors tended to dominate the precursor loading, and DBAN is known to be extremely geno- and cytotoxic to mammalian cells. At typical dilution of 90–98% for FBW and SSW recycle, the precursor loading to the head of the plant cannot be ignored. Any DBP precursors recycled need to be removed a second time during treatment. Therefore, attention should focus on occurrence and permanent removal of low MW, HPI organic matter because of its contribution to HAM and HAN formation. By permanent removal, we mean irreversible desorption from settled solids originating from FBW or SSW. Low MW and HPI organics, which were found to be the main HAN and HAM precursors in FBW and SSW, are generally difficult to remove in DWTPs. The influence of bromide cycling in treatment plants also should not be ignored because high bromide tends to selectively promote the formation of the most toxic HAMs and HANs and also other Br-DBPs. DOC and DON in FBW were higher than levels in the DWTP raw water. DOC, DON, and bromide concentrations and HAN and HAM FPs obtained for SSW were higher than those obtained for raw water. Therefore, treatment strategies should be pursued to remove precursors or preformed DBPs in backwash water.

Declaration of Competing Interest

The authors declare that they have no known competing financial interests or personal relationships that could have appeared to influence the work reported in this paper.

Acknowledgements

This work was partially funded by the National Science Foundation (CBET-1804229 and 1804255) and through the Nanosystems Engineering Research Center on Nanotechnology-Enabled Water Treatment (EEC-1449500). The authors thank National Natural Science Foundation of China (NSFC 21777031, 21577024, 50808049). Laurel Passantino provided technical editing.

Supplementary materials

Supplementary material associated with this article can be found, in the online version, at doi:10.1016/j.watres.2020.116346.

References

Ackerson, N.O.B., Machek, E.J., Killinger, A.H., Crafton, E.A., Kumkum, P., Liberatore, H.K., Plewa, M.J., Richardson, S.D., Ternes, T.A., Duirk, S.E., 2018. Formation of DBPs and halogen-specific TOX in the presence of iopamidol and chlorinated oxidants. Chemosphere 202, 349–357.

Allard, S., Tan, J., Joll, C.A., Gunten, U.V., 2015. Mechanistic study on the formation of Cl-/Br-/I-trihalomethanes during chlorination/chloramination combined with a theoretical cytotoxicity evaluation. Environ. Sci. Technol. 49 (18), 11105–11114.

An, D., Chen, Y.N., Gu, B., Westerhoff, P., Hanigan, D., 2019. Lower molecular weight fractions of PolyDADMAC coagulants disproportionately contribute to N-nitrosodimethylamine formation during water treatment. Water Res. 150, 466–472.

An, D., Gu, B., Sun, S.N., Zhang, H., Chen, Y.N., Zhu, H.F., Shi, J., Tong, J., 2017. Relationship between THMs/NDMA formation potential and molecular weight of organic compounds for source and treated water in Shanghai, China. Sci. Total Environ. 605-606, 1–8.

APHA, A.Water Environment Federation, 2005. Standard Methods For the Examination of Water and wastewater, Twenty-Firsted. APHA, Washington DC, USA.

Ates, N., Yilmaz, L., Kitis, M., Yetis, U., 2009. Removal of disinfection by-product precursors by UF and NF membranes in low-SUVA waters. J. Membr. Sci. 328 (1–2), 104–112.

Bond, T., Templeton, M.R., Kamal, N.H.M., Graham, N., Kanda, R., 2015. Nitrogenous disinfection byproducts in English drinking water supply systems: occurrence, bromine substitution and correlation analysis. Water Res. 85, 85–94.

Bourgeois, J.C., Walsh, M.E., Gagnon, G.A., 2004. Comparison of process options for treatment of water treatment residual streams. J. Environ. Eng. Sci. 3 (6), 477–484.

Chen, B., Westerhoff, P., 2010. Predicting disinfection by-product formation potential in water. Water Res. 44 (13), 3755–3762.

Chen, T., Xu, Y., Zhu, S., Cui, F., 2015. Combining physico-chemical analysis with a Daphnia magna bioassay to evaluate a recycling technology for drinking water treatment plant waste residuals. Ecotox. Environ. Safe. 122, 368–376.

Chen, W., Westerhoff, P., Leenheer, J.A., Booksh, K., 2003. Fluorescence excitation-emission matrix regional integration to quantify spectra for dissolved organic matter. Environ. Sci. Technol. 37 (24), 5701–5710.

Chiu, C.A., Westerhoff, P., Ghosh, A., 2012. GAC removal of organic nitrogen and other DBP precursors. J. Am Water Works Assoc. 104 (7), 406–415.

Chu, W.H., Gao, N.Y., Deng, Y., Krasner, S.W., 2010. Precursors of dichloroacetamide, an emerging nitrogenous DBP formed during chlorination or chloramination. Environ. Sci. Technol. 44 (10), 3908–3912.

Chu, W.H., Gao, N.Y., Deng, Y., Krasner, S.W., 2013. Formation and speciation of nine haloacetamides, an emerging class of nitrogenous DBPs, during chlorination or chloramination. J. Hazard Mater. 260, 806–812.

Chuang, Y.H., Szczuka, A., Mitch, W.A., 2019a. Comparison of toxicity-weighted disinfection byproduct concentrations in potable reuse waters and conventional drinking waters as a new approach to assessing the quality of advanced treatment train waters. Environ. Sci. Technol. 53, 3729–3738.

Croué, J.P., Violleau, D., Labouyrie, L., 2000. Disinfection by-product formation potentials of hydrophobic and hydrophilic natural organic matter fractions: a comparison between a low- and a high-humic water. ACS. Symp. 761, 139–153.

Cuthbertson, A.A., Kimura, S.Y., Liberatore, H.K., Knappe, D.R.U., Stanford, B.D., Summers, R.S., Dickenson, E.R., Maness, J.C., Glover, C., Selbes, M., Richardson, S.D., 2020. GAC to BAC: does it make chloraminated drinking water safer? Water Res. 172, 115432–115443.

Cuthbertson, A.A., Kimura, S.Y., Liberatore, H.K., Summers, R.S., Knappe, D.R.U., Stanford, B.D., Maness, J.C., Mulhern, R.E., Selbes, M., Richardson, S.D., 2019. Does granular activated carbon with chlorination produce safer drinking water? From disinfection byproducts and total organic halogen to calculated toxicity. Environ. Sci. Technol 53 (10), 5987–5999.

Dad, A., Jeong, C.H., Wagner, E.D., Plewa, M.J., 2018. Haloacetic acid water disinfection byproducts affect pyruvate dehydrogenase activity and disrupt cellular metabolism. Environ. Sci. Technol. 52 (3), 1525–1532.

Ersan, M.S., Liu, C., Amy, G., Plewa, M.J., Wagner, E.D., Karanfil, T., 2019. Chloramination of iodide-containing waters: formation of iodinated disinfection byproducts and toxicity correlation with total organic halides of treated waters. Sci. Total Environ. 697, 134–142.

Fabris, R., Chou, C.W.K., Drikas, M., Eikebrokk, B., 2008. Comparison of NOM character in selected Australian and Norwegian drinking waters. Water Res. 42 (15), 4188–4196.

Finkbeiner, P., Moore, G., Pereira, R., Jefferson, B., Jarvis, P., 2020. The combined influence of hydrophobicity, charge and molecular weight on natural organic matter removal by ion exchange and coagulation. Chemosphere 238, 124633–124642.

Golea, D.M., Upton, Jarvis, A.P., Moore, G., Sutherland, S., Parsons, S.A., Judd, S.J., 2017. THM and HAA formation from NOM in raw and treated surface waters. Water Res. 112, 226–235.

Hanigan, D., Inniss, E., Clevenger, T.E., 2013. Miex® and pac for removal of hydrophilic dbp precursors. J. Am Water Works Ass. 105 (3), 84–92.

Hanigan, D., Zhang, J., Herckes, P., Krasner, S.W., Chen, C., Westerhoff, P., 2012. Adsorption of N-nitrosodimethylamine precursors by powdered and granular activated carbon. Environ. Sci. Technol. 46 (22), 12630–12639.

Hanigan, D., Zhang, J., Herckes, P., Zhu, E., Krasner, S.W., Westerhoff, P., 2015. Contribution and removal of watershed and cationic polymer N-nitrosodimethylamine precursors. J. Am Water Works Ass. 107 (3), 152–163.

Hou, B., Lin, T., Chen, W., 2016. Evaluation of a drinking water treatment process involving directly recycling filter backwash water using physico-chemical analysis and toxicity assay. RSC ADV 6, 76922–76932.

Hu, H.Y., Du, Y., Wu, Q.Y., Zhao, X., Tang, X., Chen, Z., 2016. Differences in dissolved organic matter between reclaimed water source and drinking water source. Sci. Total Environ. 551-552, 133–142.

Hua, G., Reckhow, D.A., 2007. Characterization of disinfection byproduct precursors based on hydrophobicity and molecular size. Environ. Sci. Technol. 41 (9), 3309–3315.

Huang, H., Wu, Q.Y., Hu, H.Y., Mitch, W.A., 2012. Dichloroacetonitrile and dichloroacetamide can form independently during chlorination and chloramination of drinking waters, model organic matters, and wastewater effluents. Environ. Sci. Technol. 46 (19), 10624–10631.

Huang, H., Wu, Q.Y., Tang, X., Jiang, R., Hu, H., 2016. Formation of haloacetonitriles and haloacetamides and their precursors during chlorination of secondary effluents. Chemosphere 144, 297–303.

Huang, H., Zhu, H., Gan, W., Chen, X., Yang, X., 2017. Occurrence of nitrogenous and carbonaceous disinfection byproducts in drinking water distributed in Shenzhen, China. Chemosphere 188, 257–264.

Jiang, J., Zhang, X., Zhu, X., Li, Y., 2017. Removal of intermediate aromatic halogenated DBPs by activated carbon adsorption: a new Approach to controlling halogenated DBPs in chlorinated drinking water. Environ. Sci. Technol. 51 (6), 3435–3444.
, 2008. In: Karanfil, T., Krasner, S.W., Westerhoff, P., Xie, Y. (Eds.), Occurence, formation, Health Effects and Control of Disinfection By-Products in Drinking Water. American Chemical Society, Washington, D.C., pp. 36–50.
Karapinar, N., Uyak, V., Soylu, S., Topal, T., 2014. Seasonal variations of NOM composition and their reactivity in a low humic water. Environ Prog Sustain 33 (3), 962–971.
Kimura, S.Y., Cuthbertson, A.A., Byer, J.D., Richardson, S.D., 2019. The DBP exposome: development of a new method to simultaneously quantify priority disinfection by-products and comprehensively identify unknowns. Water Res 148, 324–333.
Komaki, Y., Marinas, B.J., Plewa, M.J., 2014. Toxicity of drinking water disinfection byproducts: cell cycle alterations induced by the monohaloacetonitriles. Environ. Sci. Technol. 48 (19), 11662–11669.
Kosaka, K., Ohkubo, K., Akiba, M., 2016. Occurrence and formation of haloacetamides from chlorination at water purification plants across Japan. Water Res 106, 470–476.
Krasner, S.W., Lee, T.C.F., Westerhoff, P., Fischer, N., Hanigan, D., Karanfil, T., Wilson, B.S., Liz, T.E., Andrews, R.C., 2016. Granular activated carbon treatment may result in higher predicted genotoxicity in the presence of bromide. Environ. Sci. Technol. 50 (17), 9583–9591.
Krasner, S.W., Mitch, W.A., McCurry, D.L., Hanigan, D., Westerhoff, P., 2013. Formation, precursors, control, and occurrence of nitrosamines in drinking water: a review. Water Res 47 (13), 4433–4450.
Krasner, S.W., Weinberg, H.S., Richardson, S.D., Pastor, S.J., Chinn, R., Sclimenti, M.J., Onstad, G.D., Thruston Jr., A.D., 2006. Occurrence of a new generation of disinfection byproducts. Environ. Sci. Technol. 40 (23), 7175–7185.
Krasner, S.W., Westerhoff, P., Chen, B., Rittmann, B.E., Nam, S.N., Amy, G., 2009. Impact of wastewater treatment processes on organic carbon, organic nitrogen, and DBP precursors in effluent organic matter. Environ. Sci. Technol. 43 (8), 2911–2918.
Krasner, S.W., Westerhoff, P., Mitch, W.A., Hanigan, D., McCurry, D.L., Von Gunten, U., 2018. Behavior of NDMA precursors at 21 full-scale water treatment facilities. Environ. Sci-Wat. Res. 4 (12), 1966–1978.
Lamsal, R., Montreuil, K.R., Kent, F.C., Walsh, M.E., Gagnon, G.A., 2012. Characterization and removal of natural organic matter by an integrated membrane system. Desalination 303, 12–16.
Liew, D., Linge, K.L., Joll, C.A., Heitz, A., Charrois, J.W., 2012. Determination of halonitromethanes and haloacetamides: an evaluation of sample preservation and analyte stability in drinking water. A J. Chromatogr. A. 1241, 117–122.
Mccormick, N.J., Porter, M., Walsh, M.E., 2010. Disinfection by-products in filter backwash water: implications to water quality in recycle designs. Water Res 44 (15), 4581–4589.
McKenna, E., Thompson, K.A., Taylor-Edmonds, L., McCurry, D.L., Hanigan, D., 2020. Summation of disinfection by-product cho cell relative toxicity indices: sampling bias, uncertainty, and a path forward. Environ Sci Proc Impacts 22 (3), 708–718.
Muellner, M., Wagner, E., McCalla, K., Richardson, S., Woo, Y., Plewa, M.J., 2007. Haloacetonitriles vs. regulated haloacetic acids: are nitrogen-containing DBPs more toxic? Environ. Sci. Technol. 41 (2), 645–651.
Phetrak, A., Lohwacharin, J., Takizawa, S., 2016. Analysis of trihalomethane precursor removal from sub-tropical reservoir waters by a magnetic ion exchange resin using a combined method of chloride concentration variation and surrogate organic molecules. Sci. Total Environ. 539, 165–174.
Plewa, M.J., Kargalioglu, Y., Vankerk, D., Minear, R.A., Wagner, E.D., 2002. Mammalian cell cytotoxicity and genotoxicity analysis of drinking water disinfection by-products. Environ. Mol. Mutagen. 40, 134–142.
Plewa, M.J., Muellner, M.G., Richardson, S.D., Fasano, F., Buettner, K.M., Woo, Y.T., McKague, A.B., Wagner, E.D., 2008a. Occurrence, synthesis, and mammalian cell cytotoxicity and cenotoxicity of haloacetamides: an emerging class of nitrogenous drinking water disinfection byproducts. Environ. Sci. Technol. 42 (3), 955–961.
Plewa, M.J., Simmons, J.E., Richardson, S.D., Wagner, E.D., 2010. Mammalian cell cytotoxicity and genotoxicity of the haloacetic acids, a major class of drinking water disinfection by-products. Environ. Mol. Mutagen. 51, 871–878.
Plewa, M.J., Wagner, E.D., 2009. Mammalian Cell Cytotoxicity and Genotoxicity of Disinfection By-Products. Water Research Foundation, Denver, CO, p. 134.
Plewa, M.J., Wagner, E.D., Metz, D.H., Kashinkunti, R., Jamriska, K.J., Meyer, M., 2012. Differential toxicity of drinking water disinfected with combinations of ultraviolet radiation and chlorine. Environ. Sci. Technol. 46 (14), 7811–7817.
Plewa, M.J., Wagner, E.D., Muellner, M.G., Hsu, K.M., Richardson, S.D., 2008b. Comparative mammalian cell toxicity of N-DBPs and C-DBPs. ACS SYM SER 995, 36–50.
Qian, W., Gao, B., Yan, W., Yang, Z., Yue, Q., 2011. Effect of pH on humic acid removal performance in coagulation-ultrafiltration process and the subsequent effects on chlorine decay. Sep. Purif. Technol. 80 (3), 549–555.
Richardson, S.D., 2011. Disinfection by-products: formation and occurrence of drinking water. Encyclopedia of Environmental Health 2, 110–136.
Richardson, S.D., Plewa, M.J., Wagner, E.D., Schoeny, R., DeMarini, D.M., 2007. Occurrence, genotoxicity, and carcinogenicity of emerging disinfection by-products in drinking water: a review and roadmap for research. Mutat. Res. 636, 178–242.
Shafiquzzaman, M., Al-Mahmud, A., AlSaleem, S.S., Haider, H., 2018. Application of a low cost ceramic filter for recycling sand filter backwash water. Water (Basel) 10 (2), 150–165.
Tan, Y.W., Lin, T., Jiang, F.C., Dong, J., Chen, W., Zhou, D.J., 2017. The shadow of dichloroacetonitrile (DCAN), a typical nitrogenous disinfection by-product (N-DBP), in the waterworks and its backwash water reuse. Chemosphere 181, 569–578.
Tobiason, J.E., Edzwald, J.K., Levesque, B.R., Kaminski, G.S., Dunn, H.J., Galant, P.B., 2003. Fullscale assessment of the impacts of recycle of waste filter backwash. J. Am Water Works Ass. 95 (7), 80–93.
Vu, T.N., Kimura, S.Y., Plewa, M.J., Richardson, S.D., Mariñas, B.J., 2018. Predominant N-haloacetamide and haloacetonitrile formation in drinking water via the aldehyde reaction pathway. Environ. Sci. Technol. 53 (2), 850–859.
Wagner, E.D., Plewa, M.J., 2017. CHO cell cytotoxicity and genotoxicity analyses of disinfection by-products: an updated review. J. Environ. Sci. 58, 64–76.
Walsh, M.E., Gagnon, G., Alam, Z., Andrews, R.C., 2008. Biostability and disinfectant by-product formation in drinking water blended with UF-treated filter backwash water. Water Res. 42 (8–9), 2135–2145.
Wang, C., Zhang, X., Wang, J., Chen, C., 2013. Characterization of dissolved organic matter as N-nitrosamine precursors based on hydrophobicity, molecular weight and fluorescence. J. Environ. Sci. 25, 85–95.
Wang, F., Gao, B., Yue, Q., Bu, F., Shen, X., 2017. Effects of ozonation, powdered activated carbon adsorption, and coagulation on the removal of disinfection by-product precursors in reservoir water. Environ. Sci. Pollut. R. 24 (21), 1–10.
Westerhoff, P., Chao, P., Mash, H., 2004. Reactivity of natural organic matter with aqueous chlorine and bromine. Water Res. 38 (6), 1502–1513.
Westerhoff, P., Herckes, P., Fischer, N., Donovan, S., Atkinson, A., Corwell, D., Brown, R., Croue, J.P., Linge, K.L., Liew, D., Lowe, A., 2019. Understanding the Source and Fate of Polymer-Derived Nitrosamine Precursors. Water Research Foundation, Denver, p. 174.
Xu, B., Gao, N.Y., Sun, X.F., Xia, S.J., Simonnot, M.O., Causserand, C., Rui, M., Wu, H.H., 2007. Characteristics of organic material in Huangpu River and treatability with the O3-BAC process. Sep. Purif. Technol. 57 (2), 348–355.
Yang, X., Shang, C., Shen, Q.Q., Chen, B.Y., Westerhoff, P., Peng, J.F., Guo, W.H., 2012. Nitrogen origins and the role of ozonation in the formation of haloacetonitriles and halonitromethanes in chlorine water treatment. Environ. Sci. Technol. 46 (23), 12832–12838.
Zeng, T., Plewa, M.J., Mitch, W.A., 2016. N-Nitrosamines and halogenated disinfection byproducts in U.S. full advanced treatment trains for potable reuse. Water Res 101, 176–186.
Zhang, Z., Chuang, Y.H., Szczuka, A., Ishida, K.P., Roback, S., Plumlee, M.H., Mitch, W.A., 2019. Pilot-scale evaluation of oxidant speciation, 1, 4-dioxane degradation and disinfection byproduct formation during UV/hydrogen peroxide, UV/free chlorine and UV/chloramines advanced oxidation process treatment for potable reuse. Water Res. 164, 114939.1–114939.11.
Zheng, J., Lin, T., Chen, W., Tao, H., Tan, Y., Ma, B., 2018. Removal of precursors of typical nitrogenous disinfection byproducts in ozonation integrated with biological activated carbon (O_3/BAC). Chemosphere 209, 68–77.